Ore Geology Reviews 101 (2018) 211–220

Contents lists available at ScienceDirect

Ore Geology Reviews

journal homepage: www.elsevier.com/locate/oregeorev

Nanoforms of gold from abandoned placer deposits of Wądroże Wielkie, Lower Silesia, Poland – The evidence of authigenic gold mineralization

Jan Wierchowiec[a], Stanisław Z. Mikulski[b,*], Arkadiusz Gąsiński[c]

[a] Institute of Geology, University of Warsaw, Żwirki i Wigury 93, 02-089 Warszawa, Poland
[b] Polish Geological Institute-National Research Institute, Rakowiecka 4, 00-975 Warszawa, Poland
[c] Institute of Ceramics and Building Materials, Postepu Street 9, 02-676 Warszawa, Poland

ARTICLE INFO

Keywords:
Gold nanoparticles
Authigenic gold
Placer deposit
Lower Silesia

ABSTRACT

Being the most recently exposed, gold grains from historical tailings of underground and surface workings offer the opportunity to study supergene transformations occurring over historic periods. In this study, gold grains were collected from the abandoned, historically mined deposits of Wądroże Wielkie at Lower Silesia.

All three distinct gold sub-types of detrital gold display surface morphotypes and internal textures of Au and Ag dissolution indicative of supergene gold modification, as well as authigenic Au nanoparticle formation and aggregation. The indicative morphotypes include nano-particulate semispherical or bubble-like gold and aggregates of bacteriomorphic gold that could be evidence for microbial gold biomineralization. SEM investigation of the microtopography and internal texture of gold grains revealed indications of post-depositional dissolution of Au-Ag alloys and redistribution of these components within the sediment. Some of seed and bubble-like growths are also embedded in clayey (kaolinite) masses within crevices suggesting that dissolution/re-precipitation processes occur at the gold grain interface.

Authigenic gold occurs as overgrowths and aggregates of nearly pure gold on a detrital Au-Ag alloy that are readily removed during transport, but are replaced by re-precipitation occurring over historic rather than geological periods.

1. Introduction

Nanogold particles have been documented in both hypogene ores (e.g. Palenik et al., 2004; Koneev, 2006; Hough and Noble, 2010) and supergene-related environments (Freyssinet et al., 2005; Reith et al., 2010; Hough et al., 2011; Zhmodik et al., 2012; Naumova et al., 2013). Nanoparticles of gold are increasingly recognized as a critical component in weathering processes (Mann, 1984; Hong and Tie 2005; Osovetsky, 2012, 2013; Craw et al., 2015), biomineralization (Lengke and Southam 2006; Shuster et al., 2015) and formation of geochemical anomalies (Cao et al., 2009). Recent research has directly recorded a natural population of gold nanoparticles in weathered environments where secondary gold mobilization and redeposition leads to the aggregation of nanometer-sized gold particles into grains, 50–100 μm in size, as well as the formation of supergene deposits (Hough et al., 2007; Fairbrother et al., 2012; Reith et al., 2012). Nanogold is usually represented by isolated particles dispersed in clay minerals and goethite, surrounding the primary deposits (Greffié et al., 1996; Hong and Tie, 2005), but under certain conditions, gold nanoparticles are able to merge with each other and compose simple or complex aggregates leading to the formation of supergene (authigenic) gold (Hough et al., 2008; Osovetsky, 2016; Shuster et al., 2017).

The phenomenon of supergene gold transformation and re-precipitation 'in situ' of authigenic gold in oxidation zones of mine dumps, gold-bearing tailings and alluvial placers was discovered in the first half of the 20 th century (Friese, 1931).

The recent study of the gold-bearing tailings from historical mining activity regions of the Lower Silesia revealed processes of gold modification, including changes in the composition of intermetallic components, grain enlargement due to gold particle adsorption, as well as the formation of authigenic gold precipitated from colloidal solutions (Wierchowiec, 2010, 2011; Mikulski and Wierchowiec, 2013). This phenomenon is of tremendous interest, because the origin of gold in weathered horizons containing tailings from mining activity is still incompletely understood.

Investigations of these human-induced (technogenic) sediments, carried out by the authors in the historical mining area of the Wądroże Wielkie (Lower Silesia) during the last few years, provided new data

* Corresponding author.
E-mail addresses: jan.wierchowiec@uw.edu.pl (J. Wierchowiec), stanislaw.mikulski@pgi.gov.pl (S.Z. Mikulski).

https://doi.org/10.1016/j.oregeorev.2018.07.009
Received 1 December 2017; Received in revised form 20 June 2018; Accepted 13 July 2018
Available online 01 August 2018
0169-1368/

and observations of nano- and micrometer-sized phases of authigenic gold, which are presented in this paper.

2. Sampling and analytical techniques

Field observations were made in and around the historical placer gold mine, where excavations reveal details of the sedimentary sequence, in which the placer gold occurs. The sample material processed in this work was collected from 1.5 to 2.5 m deep prospective outcrops, which correspond to the level of groundwater table. In order to obtain representative samples, each horizon was sampled by means of the channel chip sampling technique along its thickness and thoroughly mixed to yield a homogeneous 0.01–0.02 m^3 sample.

A total of 24 panned heavy mineral samples have been taken from the gold-bearing tailings.

Field samples were reprocessed in the laboratory by repeated careful panning of concentrates in combination with the Knelson centrifugal concentrator (McClenaghan, 2014; www.knelsongravitysolutions.com). Special care was taken to save as much of the fine gold as possible, but some extremely fine gold grains (< 10 μm) might have been lost.

All visible gold grains were separated from the reprocessed samples by hand-picking under a binocular microscope and weighed. The gold content was expressed as the number of grains counted in the sample per cubic meter (Kanasiewicz, 1982). The grains were classified according to their morphology; some were selected for further study.

Gold grains, representing different morphological classes, were investigated under the Sigma VP and Ariga 60 scanning electron microscopes (both produced by Zeiss, Germany) in order to study the nano- and micro-morphology. Energy-dispersive detectors (XFlash 6/10 and X/Flash 6/30) were used to obtain the semiquantitative chemical data and mapping of elements. Gold particles were mounted with sticky carbon tape on aluminium holders and placed directly into the instrument without any addition of conductive coating. Gold grains previously investigated under a scanning electron microscope were subsequently embedded in epoxy resin, polished and viewed under reflected polarized light. The BSE imaging and EDS analysis, including mappings, were performed on these thin sections. The operating conditions were: 20 kV accelerating voltage, 150 μm aperture size with 20 nA regulated current. Quantitative chemical analyses (EMPA) of gold grains were conducted by means of the CAMECA SX Five electron microprobe equipped with five wavelength-dispersive spectrometers. Representative gold grains were analysed for Ag, As, Au, Bi, Cu, Hg, Pb, Pd, Pt, Tl and Zn. Pure metals (**Au**Mα where: **Au** – analysed element and Mα – measurement line, **Pd**Lα, **Pt**Mα), chalcopyrite (**Cu**Kα), ZnAs (**Zn**Kα, **As**Lα), Bi_2Te_3 (**Bi**Mα), Tl (**Tl** Mα,), crocoite (**Pb**Mα), HgTe (**Hg**Mα) and Ag_2S (**Ag**Lα) were used as standards. The operating conditions for EMPA were: 15 kV accelerating voltage, 10 nA primary beam current, 25 sec counting time.

Mappings were made for representative grains to check for changes in chemical composition. The element contents of mineral grains smaller than the beam spot (many particles < 1 μm and porous, polymorphic aggregates) were estimated from relative major element contents by subtracting the elements of the host mineral. SEM and microprobe analyses were performed at the Warsaw University of Technology (Poland).

3. Geological setting and mining activity

3.1. Historical mining activity in the region

Gold-bearing tailings from historical mining activities are quite widespread in the Wądroże Wielkie area, a region with a long history of mining. As early as in the 14th century, gold was recovered from Neogene eluvial/alluvial sediments and hydrothermal quartz veins in the vicinity of Mikołajowice and Wądroże Wielkie villages (Figs. 1 and 2).

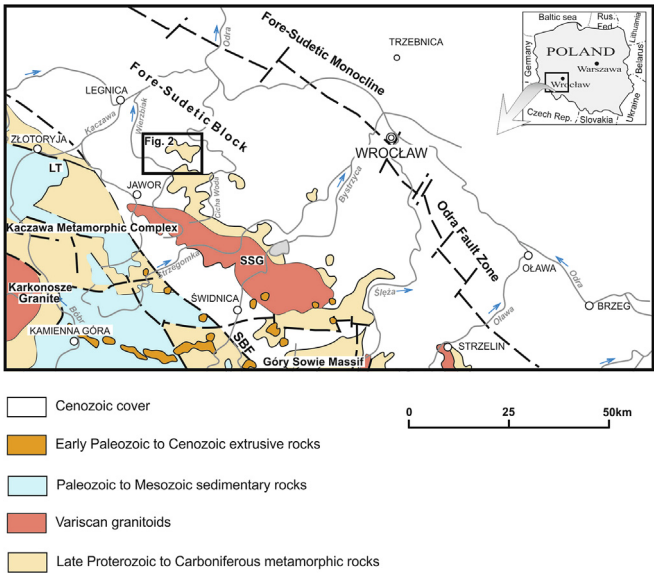

Fig. 1. Generalized geological-structural map of Lower Silesia (after Sawicki and Teisseyre, 1978) with location of historical mining activity in the Wądroże Wielkie region. GT – Grodziec Trough, ISF – Intra Sudetic Fault Zone, LT – Leszczyna-Jerzmanice Trough, LwT – Lwówek Trough, OSD – Orlica-Śnieżnik Dome, SBF – Sudetic Boundary Fault, SSG – Strzegom-Sobótka Granite Massif, VU – Vrbno Unit, WW – Wądroże Wielkie gneisses, WG – Wleń Graben, ZG –Żulowa Granite, ZL – Złotoryja-Luboradz Unit.

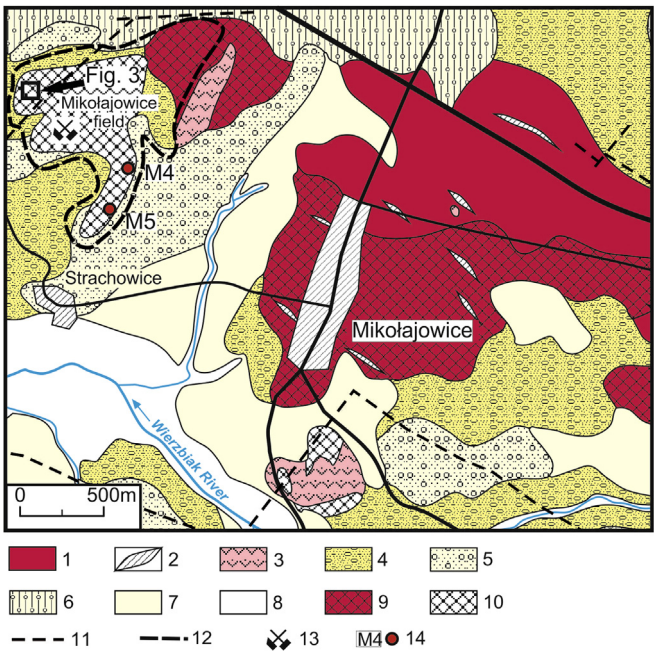

Fig. 2. Simplified geological map (compiled after Berezowska and Berezowski, 1979) showing the approximate extent of historical mining activity in the Wądroże Wielkie region and location of the sampling sites (outcrops); 1 – granite gneisses (Precambrian), 2 – quartz vein (Carboniferous), 3 – basalt (Neogene), 4 – kaolin-rich clastic sedimentary series (Tertiary), 5 – glaciofluvial sand and gravel (Saalian), 6 – till (Saalian), 7 – fine- to coarse-grained eluvium and colluvium, 8 – alluvial sediments (Weichselian to Holocene), 9 – kaolin-dominated regolith, 10 – field with heaps of post-mining material, 11 – hypothetical fault, 12 – inferred extent of historical mining field 13 – historical gold mine, 14 – sampling site (location of the outcrop section).

According to historical records, in 1343 there were 15,000 miners, extracting between 1500–3000 g of gold daily (Quiring, 1913;

Domaszewska, 1964). Gold mining declined at the turn of the 14th century, mainly due to the depletion of surface gold resources and the lack of technology to prevent flooding of deeper workings.

In the 18th and 19th centuries, the area was encompassed by German territorial borders and the Germans attempted further mining of the goldfields, but they were also unable to address problems involving dewatering of the richest bottom parts of the placers.

Efforts to resume mining were then made up until the 20th century. In 1924, Scholler & Co. from Frankfurt (Germany) initiated a new phase of gold exploration in the area. Their drilling works found scattered occurrences of gold at the bottom of the coarse-grained eluvial/alluvial sediments. Gold was mainly associated with pyrite and pitted vein quartz. The chemical analysis indicated grades of about 1.5 g/t (Zöller and Heuseler, 1926), which were considered too low for further evaluation. However, the recent analysis of the medieval tailings returned gold contents of up to 5 g/t (Hefton, 1999). These preliminary investigations showed that such technogenic sediments still contain significant amounts of gold.

3.2. Background geology

The study area lies in the crystalline basement of the Fore-Sudetic Block (Fig. 2), at the north-eastern edge of the Bohemian Massif and is underlain mainly by Precambrian granite gneisses (Grocholski, 1986; Cwojdziński and Żelaźniewicz, 1995). The typical granite gneiss of the Wądroże Wielkie massif is a grey, coarse-grained rock, composed of bluish quartz, tabular grey-white feldspars, and aggregates of dark mica and remnants of black schist.

Selective chemical weathering of granite gneisses, occurring on the top of the Wądroże Wielkie Massif, controlled by tectonics, has led to the formation of a characteristic etchplain-type landscape, which was partly buried under Cainozoic clastic sediments and relics of regoliths (Migoń, 1997; Badura and Przybylski, 2004). Regolith profiles show gradual transition from poorly weathered host rock to totally kaolinized, structureless sediment at the surface. Veins of quartz, of different thickness, which formerly cut the granite gneisses, accompany these kaolin-reach regoliths.

Primary mineralized zones consist mainly of quartz, with minor pyrite, chalcopyrite, feldspars, and hematite (Berezowska and Berezowski, 1979). Sulfides are preserved in massive quartz and commonly are goethitized on grain margins and fractures. Native gold is rare, occurring mostly as sub-microscopic blobs in pyrite and as free, fine (< 0.1–0.2 mm) grains of gold in association with pitted quartz with clayish material (Zöller and Heuseler, 1926; Grodzicki, 1966). This gold-bearing pyrite has only been observed in fresh material from the post-mining heaps. No sub-microscopic gold was detected within the sulfides down to the microprobe detection limit of about 0.1 wt% (Wierchowiec, 2010).

The gold-bearing clastic sediments in the Wądroże Wielkie area can be grouped into the following two categories: 1) Eluvial and colluvial, coarse, loosely cemented gravels and gravely sands with a kaolinite-rich sandy matrix of the Tertiary and Quaternary age. In these sediments, irregular placer gold concentrations may reach 0.1–0.3 g/m^3 (Quiring, 1913);

2) Late Quaternary low-grade auriferous alluvial deposits, present in the Wierzbiak River valley and its tributaries. Their gold content is of the order of 0.08–0.12 g/m^3 (Grodzicki, 1966). In waste heaps of sand left behind after sluicing and panning, a residual gold content of 0.02–0.20 g/m^3 is still present (Wierchowiec, 2010).

3.3. Technogenic gold-bearing sediments

In the post-mining technogenic cross-sections, the 'normal' composition of the gold-bearing layer is complicated by pits filled with mixed artificial material. In part of these sediments, there are various layers of alluvium or fragments of bedrock, interlayered with organic remnants and peat, while the upper section consists mostly of sand. The sandy sediments contain high percentages of kaolinite.

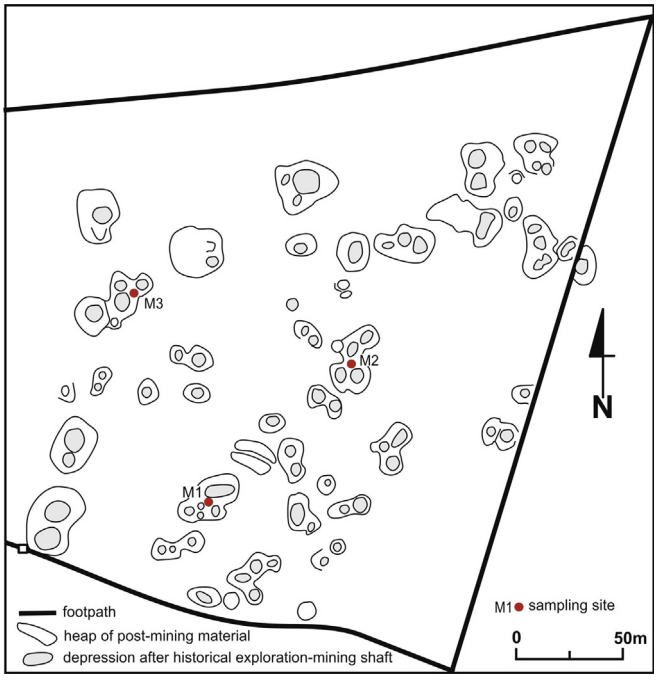

Fig. 3. Detailed locality map showing the remnants of shafts and surrounding heaps of post-mining wastes in the area north-west of Mikołajowice (modified after Wierchowiec, 2010), and the sampling sites (outcrops) for this study. The location is outlined in Fig. 2.

The basic stratigraphic sequence at the Wądroże Wielkie historic mining area, from bottom to top, consists of a loosely cemented light-coloured eluvial-colluvial very poorly sorted mixture of gravels and gravely sands with a kaolinite-rich sandy matrix of the Tertiary and Quaternary age. Large amounts of these sediments had been processed in the past. Remnants of mining activities are particularly abundant in the area of Mikołajowice (Fig. 2).

The remains of former mining activities are preserved here as fields with depressions after prospecting and exploration shafts (Pingenfelds) and heaps of post-mining material (Fig. 3). The post-mining debris occurs as 1–3 m thick irregular heaps of poorly rounded quartz gravel and angular clasts of vein quartz (80–95%), minor quartz and siliceous schists (Fig. 4). Their lower parts are commonly formed of matrix-supported diamictons, whereas the upper parts are composed of layers of sandy silts and clays with single cobbles and pebbles. All this material has been cemented, to some extent, by a kaolinite-rich matrix. Groundwater composition is controlled by pH and Eh changes during the wet and dry season of moderately cold climate, which is typical for the mountain sides in central Europe. Lateral migration of gold depends dominantly on the chemical characteristic in surrounding environments. The pH of groundwater ranges from 5 to 8 under supergene conditions (Fe-Ti oxyhydroxides and kaolinite commonly occur). In groundwaters dominate ions are SO^{-2}, HS^{-}, as well as humid acids.

Technogenic deposits locally contain high amounts of placer gold but are generally small in extent, with the best gold grades found in pockets of virgin gravels (up to 0.2 g/m^3), and the lowest gold grades found in fine tailings. In this locality, irregular placer gold concentrations may reach 0.1–0.3 g/m^3 (Quiring 1913; Wierchowiec 2010).

4. Results

Three visibly distinct gold sub-types are identified based on their overall morphology: 1) flaky gold, flattened, two dimensional (2-D) shaped; 2) reshaped, multiply refolded flakes; 3) craggy, irregular,

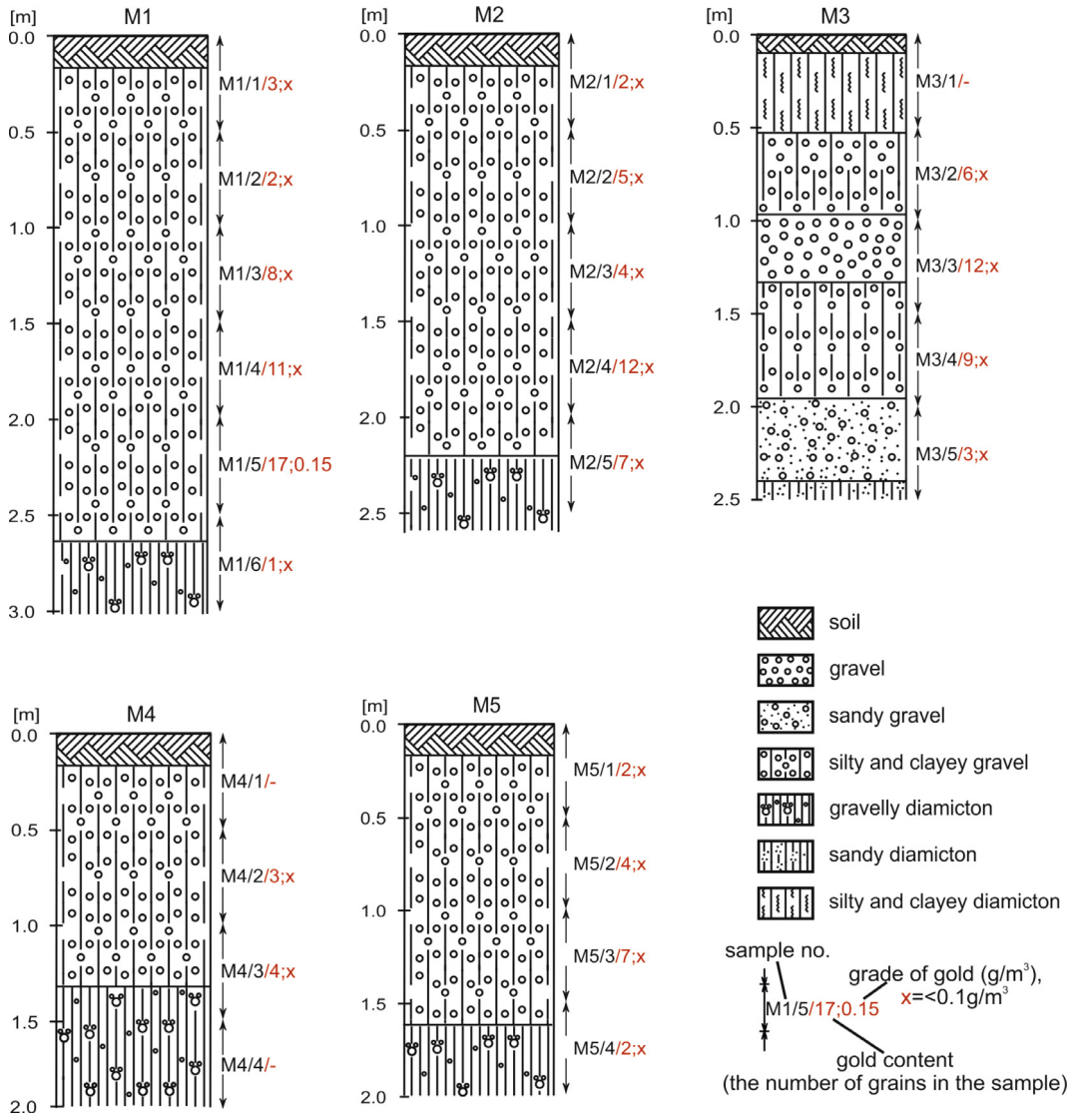

Fig. 4. Schematic outcrop sections of the representative gold-bearing deposits of the Mikołajowice historical mining field showing the location of samples presented in Figs. 5–9; the locations of the outcrop sections are shown in Fig. 2 (outcrops M4, M5) and 3 (outcrops M1-M3).

three-dimensional (3-D) shaped grains. The following section documents dissolution textures in each sub-type and supergene transformation features, which characterize them.

4.1. Flaky gold

Flaky, recycled gold is generally fine grained, ranging within 0.05–0.8 mm in size, and over 70% of particles are within 0.1–0.5 mm. Most flakes have flat and smooth surfaces with numerous irregular cavities and discontinuities, and the edges of individual particles are moderately to well-rounded (Fig. 5A).

In this gold sub-type, remnants of crystal shapes are still preserved on the surface of some particles, especially in topographically low areas (concavities) that were protected against abrasion (Fig. 5B). In detail, anhedral crystal boundaries and other discontinuities in the original gold particles have been preferentially etched by the dissolution of particle surfaces, to expose the internal grain texture with crystalline appearance.

Dissolution pits, embayments and valleys on flaky grain surfaces are often filled with clayey masses and ferruginous material, composed of Al, Si, O and C, mixed with small amounts of Fe, Ti oxyhydroxides (SEM–EDS analysis) (Fig. 5C).

In addition, delicate and crystalline exterior overgrowths protrude from surface and infill protected cavities. Micrometer-scale overgrows have coalesced in places to form initial plates, some of which are elongated with irregular ribs (Fig. 5D). The individual plates are made up of microcrystalline gold with sharp crystal boundaries. More rarely, the abraded and etched surfaces have been coated with these nano- to μm-scale gold plates (Fig. 5E).

The flaky grains also display no crystalline gold morphotypes that occur either on open surfaces or in protected cavities: bud-like protrusions and bubbly forms, as well as compact flattened aggregates or complex, porous aggregates with coral-like appearance (Fig. 5F, G, H). All of these inferred gold forms are well preserved with no physical deformation.

Typically, gold aggregates in cavities merge into extended irregular layers, forming a sheet-like gold morphotypes. On these newly formed layers, the individual bubbles of gold often remain clearly distinguishable. Most of layers are in direct contact with grain surfaces, some appear to be embedded within polymorphic clay-ferruginous coats (Fig. 5F).

Coral-like gold morphotypes are made up of conglomerates of small buds and bubbles up to 200 nm in diameter, in which separate buds appear to have nucleated from the previous buds resembling

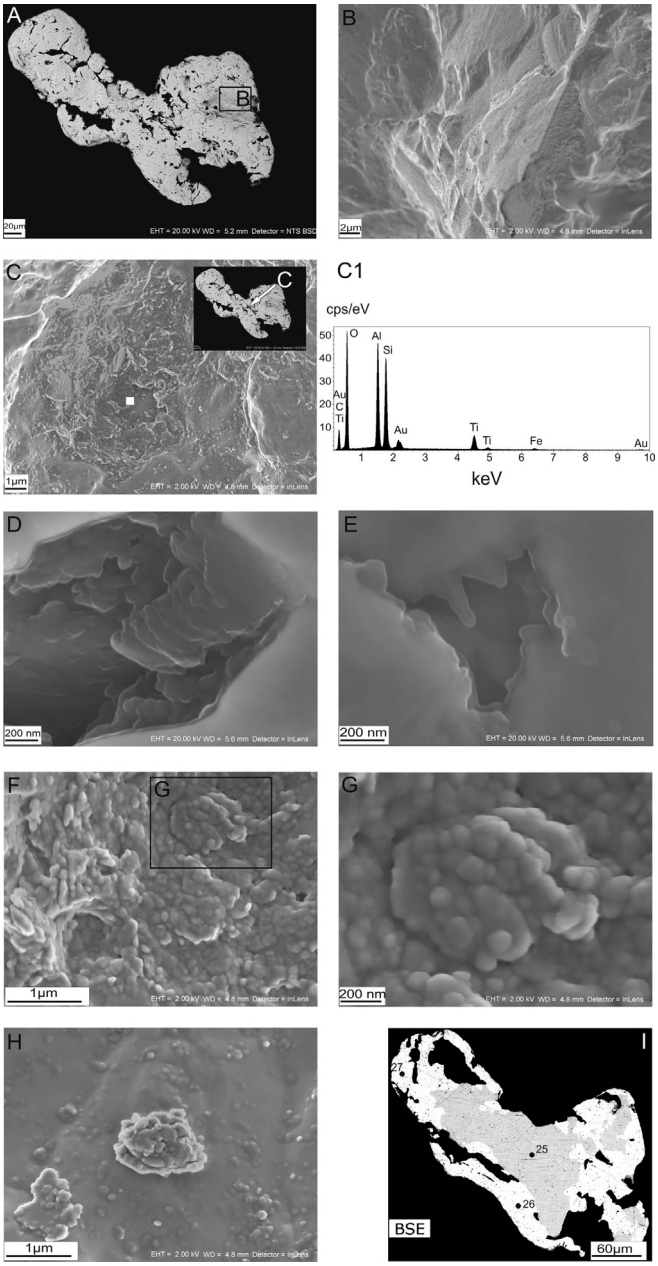

Fig. 5. Secondary electron micrographs (SEM) of flaky gold grain surfaces from the Mikołajowice field and a back-scattered electron (BSE) image of a polished section (micrograph I) showing: (A) the size and typical morphologies; (B) the highly textured grain surface (A, inset); (C) the SEM micrograph of a concavity containing nanophase gold; white square inside the concavity, represents the analytical spot of EDS data shown on graph C1; (D, E) high-resolution SEM micrographs of crystalline initial plates infilling protected cavities. Note the sharp and irregular ribs of individual plates; (F) no crystalline gold morphotypes occurring in the concavity; (G) a flattened aggregate of bud-like and bubbly forms (F, inset); (H) porous aggregates with coral appearance; (I, section of particle shown on micrograph A) an irregular, Ag-poor primary core (dark grey) discontinuously surrounded by a fine rim (light grey); numbered black dots correspond to microanalyses in Table 1.

bacteriomorphic gold. The space between separate bubbles is filled with binding masses of gold, consisting of nearly pure gold (> 99 wt%). Because of the small particle size and the presence of Ag-bearing gold in the background, only a qualitative analysis was possible.

The detailed analyses of electron micrographs show that the individual buds and bubbles of gold are in varying degrees of contact with their parent grain surface. Some nanoparticles scarcely touch the surface of the particle, while others have grown into the surface layer of gold at a predetermined depth (Fig. 5G). This fact indicates the time difference of nanoparticle deposition on the surface of a gold grain. Likely, single nanoparticles immersed over time in the newly formed layers of gold. The most ancient ones of them are probably not distinguishable, being overrun by the layer of authigenic gold.

Internally (in polished sections), flaky gold grains are optically zoned with internal patches of nearly pure, silver-depleted gold in the relict primary Ag-rich cores and external high purity rims and coatings (Fig. 5I). The boundaries between Ag-bearing and Ag-poor gold are sharp at the micron scale. Ag-depleted rims generally follow corrosion pits on the surface of particles and prefer directions related to crystalline features.

All the cores are alloys of gold and silver, with Hg, Bi, Pt and As, occurring as trace amounts (Table 1).

Rims are typically composed of low-Ag gold (< 0.01–2.87 wt%, the mean of 20 analyses: 0.67 wt% Ag), whereas the composition of cores is bimodal, with medium-Ag cores, containing < 20 wt% Ag (the average of 11 analyses: 17.64 wt% Ag) or Ag-rich (electrum) cores with silver content in the alloy, ranging from 24.63 to 28.96 wt% (the average of 9 samples: 26.75 wt%).

4.2. Reshaped flakes

The reshaped gold sub-type occurs predominantly as repeatedly folded flakes forming discoidal 'sandwiched' gold grains (Fig. 6A) or elongated cigar-shaped particles produced by rolling of flattened flaky particle (Fig. 6B). Other gold forms that are included in the reshaped gold category are stubby grains. These multiply refolded particles produced by folding of highly flattened grains are short (typically 0.4 mm long by 0.3 mm wide) and not flattened (Fig. 6C). Occasionally, some reshaped particles have fine-grained rounded to angular quartz detritus inclusions.

Scanning electron microscopy revealed numerous subcirculars to meandering pits and valleys on the surfaces of reshaped gold grains. These concavities are filled with polycrystalline layered crystal growth of gold (Fig. 7A), as well as a number of gold nanoparticles and sub-µm size gold aggregates (Fig. 7C) that are often associated with the vermiform clayey masses, consisting of Al, Si, O, C, Fe and Ti, based on an SEM–EDS analysis (Fig. 7B).

The individual gold nano-particles are between 50 and 200 nm in size and have a bud- or seed-like morphology (Fig. 7D, E). Most of these nanogold particles are in direct contact with grain surfaces (budding from crystalline grain surface); some are also dispersed throughout the clayey material (Fig. 7B). Seed-like nanoparticles did not display clear crystalline faces, suggesting that the particles were in an early stage of aggregation. Other commonly encountered features of seed-like gold are the distribution patterns of seed overgrowths (Fig. 7E), resembling an electro-deposited gold film, as shown by Kim et al. (2009).

On the individual grains of gold, distinct forms of dissolution can be seen, which reveal their crystallographic forms. Abraded surfaces of plate-like gold morphotypes commonly show a tabular, terrace-like texture, with a relief of a few microns, possibly representing former bladed intergrowths (Fig. 7A). Unmodified, crystallographic overgrowths are rare. They are characterized by a size of 50 – 100 nm, a smooth surface and an extremely pure composition (Fig. 7C).

Both the plate-like gold overgrowths as well as the conglomerates of bud- and bubble-gold display dissolution textures that expose the crystal boundaries of individual gold crystals (Fig. 7A), marking the nano-particle boundaries in the aggregates (Fig. 7D, F).

Rare mineral inclusions are partly coated by aggregates of nano- to µm bud-like gold or layers of plate-like gold overgrowths (Fig. 7A, D).

Internally, reshaped gold grains are compositionally inhomogeneous with internal veinlets and patches of nearly pure, silver-depleted gold in the relict primary Ag-rich cores and external high purity rims and coatings with a characteristic sponge-like texture

Table 1
Representative EMPA analyses (wt. %) in polished sections of the gold grains from the post-mining sediments of the Mikołajowice field. For the locations of the analyzed spots, see Figs. 5, 6 and 8.

Type of gold grain	Analysis No.	Position	AuMα	AgLα	HgMα	PtMα	CuKα	BiMα	AsLα	Total
flaky	1	core	72.975	26.137	0.245	0.019	0.000	0.046	0.004	99.426
	4	rim	98.460	1.724	0.040	0.000	0.000	0.113	0.049	100.387
flaky	9	core	70.669	28.960	0.070	0.000	0.000	0.116	0.018	99.841
	13	rim	98.651	0.716	0.000	0.000	0.000	0.000	0.017	99.385
	14	core	82.290	16.499	0.095	0.000	0.000	0.062	0.000	98.946
flaky	16	core	98.267	0.467	0.000	0.005	0.000	0.075	0.014	98.828
	17	rim	96.769	2.874	0.112	0.000	0.000	0.000	0.000	99.755
stubby	19	core	75.210	23.909	0.337	0.003	0.001	0.030	0.000	99.489
	20	rim	96.014	3.256	0.000	0.000	0.025	0.000	0.002	99.298
	21	core	68.524	30.459	0.112	0.018	0.000	0.046	0.020	99.180
craggy	22	rim	96.493	2.781	0.000	0.011	0.000	0.000	0.002	99.287
	24	rim	98.223	1.270	0.000	0.000	0.000	0.039	0.023	99.554
	25	core	82.399	17.871	0.000	0.000	0.000	0.043	0.000	100.313
flaky	26	rim	98.483	0.169	0.031	0.044	0.000	0.000	0.017	98.744
	27	rim	100.071	0.074	0.000	0.007	0.000	0.000	0.009	100.161
craggy	28	core	87.408	12.290	0.000	0.000	0.000	0.035	0.025	99.758
	29	rim	98.033	0.914	0.000	0.048	0.000	0.033	0.000	99.027
	30	core	81.350	18.542	0.000	0.023	0.053	0.059	0.006	100.033
craggy	32	rim	89.841	6.325	0.000	0.000	0.000	0.036	0.001	96.203
	33	rim	98.674	1.221	0.000	0.009	0.000	0.014	0.002	99.919
	35	core	80.073	19.189	0.000	0.000	0.000	0.086	0.000	99.349
flaky	36	rim	96.887	1.431	0.035	0.000	0.000	0.092	0.004	98.449
	37	rim	98.507	0.121	0.040	0.000	0.000	0.000	0.028	98.696
flaky	40	core	98.638	0.186	0.000	0.000	0.001	0.048	0.021	98.894
	41	rim	73.180	24.634	0.065	0.000	0.004	0.033	0.000	97.916
	42	core	89.503	9.077	0.046	0.000	0.000	0.114	0.000	98.740
stubby	43	core	74.389	24.687	0.000	0.016	0.000	0.068	0.000	99.160
	44	rim	94.275	3.003	0.000	0.001	0.000	0.000	0.000	97.279
	45	core	76.094	23.466	0.201	0.000	0.000	0.097	0.022	99.880
craggy	47	core	75.751	23.188	0.175	0.000	0.000	0.000	0.017	99.131
	50	rim	96.252	3.729	0.000	0.000	0.000	0.000	0.000	99.982

(Fig. 6D).

The grain chemistry of the studied gold shows that silver is the only element present in high concentrations (Table 1). The cores of gold grains are relatively silver-rich, with variation in Au-Ag concentrations from 9.1 to 24.7 wt% Ag. Rarely, the grain cores also contain Hg (< 0.3 wt%) and trace amounts of Pt, Cu, Bi and As.

Rims are composed of high-purity gold (up to 99.0 wt%), with a maximum silver content of 3.3 wt% in hotspots. Concentrations of other metals in rims, including Hg, were below the level of detection.

4.3. Craggy grains

The craggy grains, in contrast to the widespread flaky or reshaped (physically deformed) grains representing not recycled gold, are

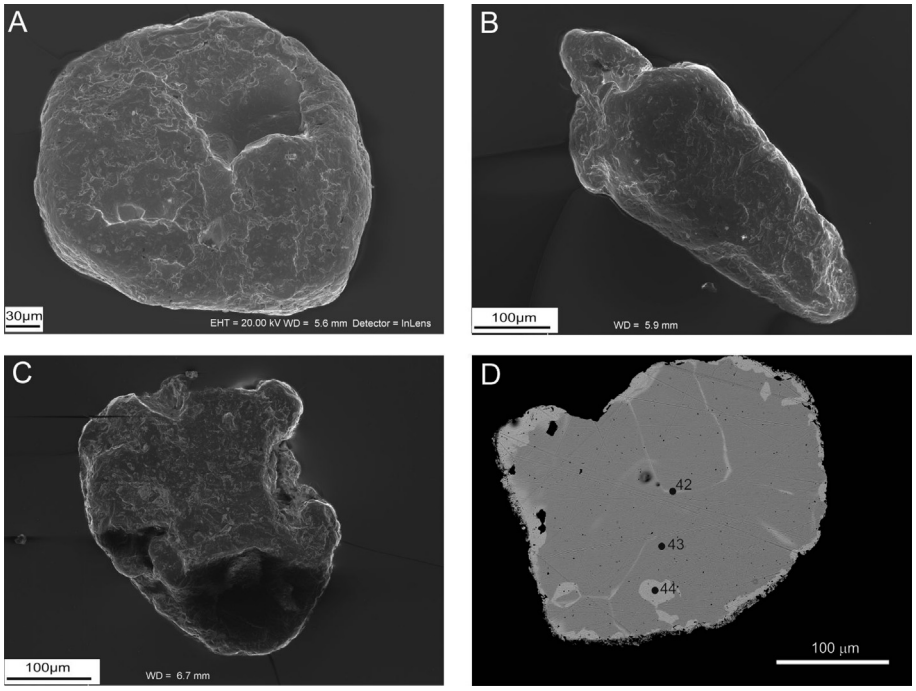

Fig. 6. SEM micrographs of the typical reshaped gold particles from the Mikołajowice field showing (A, B, C) the size and typical morphologies of multiply refolded particles. A BSE image of sectioned gold particle shown on micrograph C with an irregular Ag-rich core (dark gray), internal veinlets and patches (light gray) and the external sponge-like zone (rim) of pure gold (D).

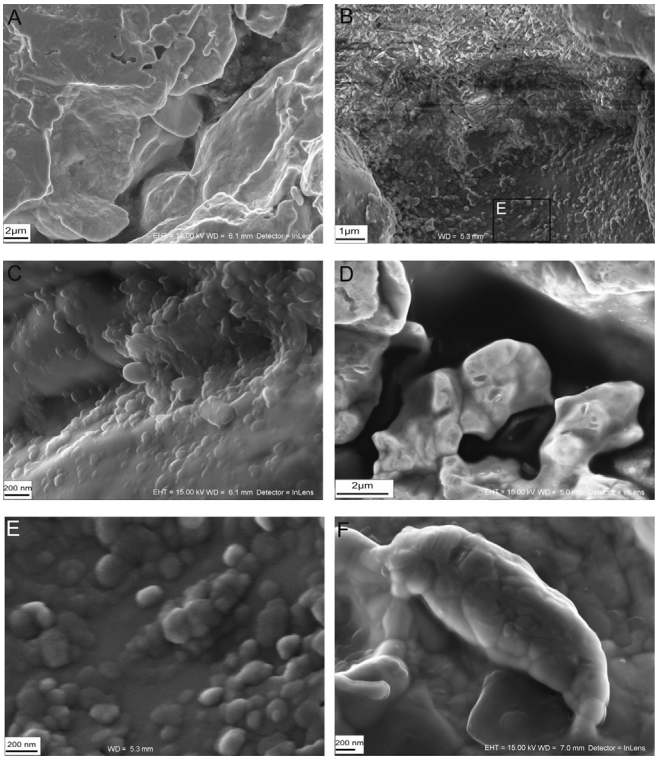

Fig. 7. SEM micrographs of concavities filled with polycrystalline layered crystal growth of gold (A); Au nano-particles associated with vermiform clayey material (B). Note that some particles are partially embedded within clay. High resolution SEM micrographs of nano- and sub-μm size Au aggregates (C); nano-particles of gold with different morphologies (D, E); mineral inclusion (D, white arrow) partly coated with aggregates of bud-like gold; dissolution textures marking the nano-particle boundaries in the aggregates (F).

typically irregularly-shaped (craggy, lobate forms) and microcrystalline in appearance, with straight grain boundaries that have suffered negligible deformation (Fig. 8A, B). These gold particles, three-dimensional in shape, usually fall within the 0.2–0.5 mm size range and bear abundant dissolution features (pits, irregularly-shaped cavities or meandering valleys), occurring directly adjacent to precipitation features, i.e., bud-like bacteriomorphic or seed-like gold, overgrowths of microcrystals and agglomerates of gold nanoparticles (Fig. 9A–E).

The dissolution of the gold-enriched grain rim surface has locally revealed the original internal crystal structure of the gold particle with nano- to microcrystalline (from 100 nm to 10 μm) growths, forming a stepped microrelief (Fig. 8A, 9C).

The cavernous surfaces are precisely the dissolution textures, as confirmed by the equality of composition of massive, crystalline and 'corroded' areas. This characteristic corrosion sculpture seems to be formed by the preferential dissolution of the more soluble silver from enriched zones in processes that are controlled by the grain texture and chemical composition.

The craggy grains also display delicate nano- to μm sized budding-textures that protrude from the walls of topographic lows in the original grain surfaces (Fig. 9B), as well as cluster gold textures that are reminiscent of bacteriomorphic gold (Fig. 9E). These complex aggregates were observed exclusively in protected areas and appear to form via the agglomeration of hundreds of individual nanometre-sized semispherical gold particles.

Rarely, the aggregates of nano- to μm-Au particles form chains of buds (a bacteriomorphic budding morphotype), in which each bud appears to have nucleated from the previous one (Fig. 9F).

In addition, especially in irregularly-shaped cavities, precipitation features of polycrystalline layer by layer overgrowths with plate-like shapes are common, and these locally span across deeply etched pits and valleys in the grain surfaces (Fig. 9G).

Earlier-formed microcrystalline growths are in turn commonly overgrown by younger layers of gold, forming a comb-like gold morphotype. This may be a progressive process in a single overgrowth generation. However, there is also evidence for more than one generation of exterior overgrowths in some deeply etched parts of grains, where an earlier generation of plate-like gold has been abraded and then overgrown by a later generation of irregularly-shaped plates of gold (Fig. 9G).

Analyses of representative craggy gold grains show that all they consist of variable proportions of gold and silver (Table 1). In polished sections (Fig. 8C, D), this type of particles has a distinct but irregularly-

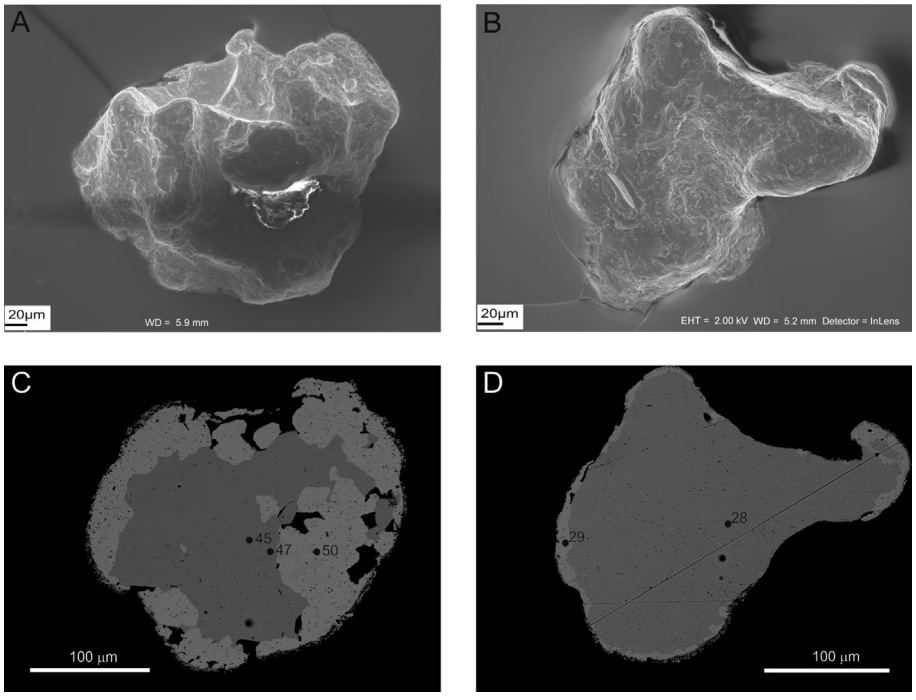

Fig. 8. SEM micrographs (A, B) and BSE images of the polished section of gold particles shown on the micrographs (C, D) of representative craggy grains from the Mikołajowice field. Typical irregularly shaped forms, microcrystalline in appearance (A, B); particles with well-defined irregular cores (dark gray) surrounded by porous, high purity Au rims (light gray) (C, D).

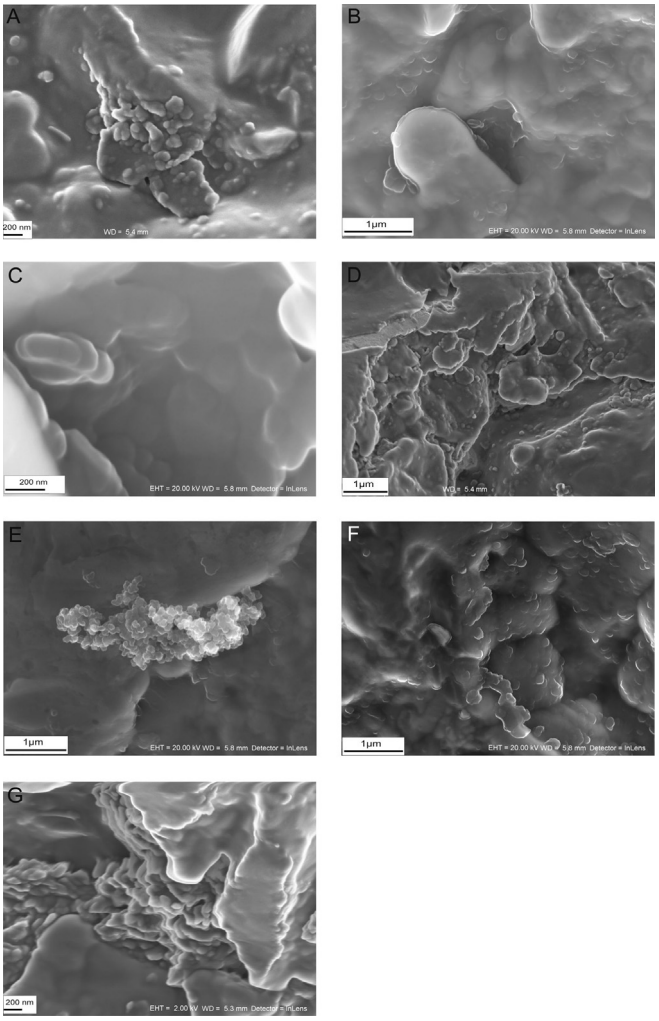

Fig. 9. High-resolution SEM micrographs of individual and aggregated nano-particulate gold, covering craggy grain surfaces (Mikołajowice field). Bud-like bacteriomorphic gold (A, B); seed-like gold (C), overgrowths of microcrystals (D); cluster gold, reminiscent of bacteriomorphic gold (E); aggregates of Au nano-particles forming chains of buds (F, white arrow); polycrystalline layer by layer overgrowths with plate-like shape in a deeply etched pit (G).

shaped core zone, consisting of silver-bearing gold (12.3–30.5 wt% Ag) and high purity rims, spots and external coatings with variable silver contents (0.9–6.3 wt%).

5. Discussion

All the considered morphological gold varieties in the studied sediments bear traces of dissolution/re-precipitation and reveal particularities of authigenic gold morphology and grain textures, like those described earlier by Wierchowiec (2010).

In some cases, it is difficult to establish the true nature of gold particle morphology (microtopography) and their internal heterogeneous texture. On many grains, there are both traces of dissolution and traces of growth. These confirm the cyclical character of the physicochemically unstable environment of post-mining, human-induced sediments with multiple episodes of gold dissolution and re-precipitation.

However, independent of the predominance of dissolution or re-precipitation processes, one characteristic feature of the distinguished gold grain sub-types is the presence of a nanogold phase. Nanogold particles are actually found in many geological environments as a component of colloidal or ionic solutions. Nano-particulate gold precipitates from colloidal and other solutions at geochemical barriers of different types, leading to the formation of geochemical anomalies and high-grade supergene accumulations (Hough et al., 2011; Craw et al., 2015). During chemical migration, nanophase colloids can be absorbed due to changes in pH and Eh by various minerals, including placer gold (Shuster and Southam, 2015; Kirillov et al., 2016; Shuster et al., 2017).

In polished sections, most of the studied gold grains are optically zoned with internal veinlets and patches of nearly pure, silver-depleted gold in the relict primary Au-Ag cores and external high purity porous rims and coatings. Silver-depleted domains occurring along solution veinlets within the grains indicate that weathering fluids penetrated the gold grains from outside through micro- or nano internal discontinuities or crystallographic planes and leached silver (Desborough, 1970; Knight et al., 1999; Oliveira and Larizzatti, 2006). Silver-depleted rim of authigenic gold grains was commonly observed in technogenic sediments in the Wądroże region. It was due to gold and silver mobilization and redeposition, controlled by pH and Eh changes in groundwater table composition during the wet and dry seasons. Lateral migration of gold depends dominantly on its occurrence in the mineralized parent rock (quartz, clay minerals with dominant kaolinite, Fe-Ti oxyhydroxides; pH range 5–8), and, under supergene conditions gold was dissolved as thiosulphates complexes – $Au(S_2O_3)_2^{3-}$ or, under more reduced conditions, as HS^- and humic acid complexes in a chloride-poor surficial environment (Webster, 1986). However, complexing by $S_2O_3^{-2}$ results in poor or no partitioning of Au and Ag, so the high purity rims are rather results of HS^- and humic acid complexes, transporting agents for the pure gold overgrowths (Webster and Mann, 1984; Clough and Craw, 1989; Kerr and Craw, 2017).

This phenomenon has been used in nano-industry to produce thin films, possessing novel nanoporous textures with unique properties (Cobley and Xia, 2009).

In favourable supergene conditions, assemblages of younger seed-like gold, bud-like bacteriomorphic gold and complex aggregates of coral-like gold were precipitated on the inside of the dissolution voids and cavities.

Furthermore, it is not clear as to when the re-precipitation of gold occurred in relation to the time of the deposition of host strata, nor it is presently possible to determine with certainty the geochemical environment of alloy dissolution and secondary re-precipitation of gold.

The inclusions of silica and aluminosilicates, observed on the surface of gold grains, may have been pressed into the external layers of a particle by physical reworking. However, mineral inclusions are partly coated by plate-like gold overgrowths or aggregates of bud-like gold (Fig. 7A, D). These would have been destroyed if the inclusions were pressed into the surface by post-depositional physical processes. Hence, the morphotypes of gold being authigenic in origin as identified in this study, can be interpreted as recent (occurring over historic periods) precipitation and aggregation features.

Clayey masses and ferruginous material observed within concavities of studied grains contain a gold nanophase and show similarities to polymorphic layers observed on gold grains from Australia (Fairbrother et al., 2012) and New Zealand (Clough and Craw, 1989; Reith et al., 2012). These observations suggest that active chemogenic and bacterially mediated processes might drive the formation of nano-particulate gold and other gold morphotypes identified in this study.

The presence of nano- to microphase gold embedded, in the fine-grained assemblages of clayey masses, and the lack of any signs of grain surface abrasion confirmed that especially seed-like gold, bud- and babble-like bacteriomorphic gold, as well as complex aggregates of cluster and coral-like gold must have formed ‘in situ’, i.e. they are authigenic in origin.

Likely, aggregation textures develop through repeated nucleation of gold nano-particles to form semispheroidal bud- and bubble-like gold, with further aggregation leading to aggregates with cluster and coral appearance similar to models presented by Falconer and Craw (2009),

Osovetsky (2016) or Kerr and Craw (2017).

Typically, coral-like gold aggregates merge into extended irregular layers, forming a sheet-like gold morphotype, where the individual buds often remain clearly distinguishable (Fig. 5F, G). Most of these layers are in direct contact with grain surfaces, some appear to be embedded within the polymorphic clay-ferruginous coats. These results confirm the outcome of the earlier work by Reith et al. (2012), who studied a sequence of placer deposits along the southern coast of New Zealand.

As reported by Groen et al. (1990), both the plate-like gold overgrowths as well as the aggregation textures may form as a consequence of self-electrorefining process and represent authigenic gold precipitated from solution on the surface of primary gold grains. The Ag-Au alloy is electrochemically dissolved, and the pure phase of 'new' authigenic gold immediately precipitates on the surface of the grain that serves as a nucleating site for internally (from the primary Ag-Au alloy) sourced gold.

Self-electro-refining could increase gold fineness as rims on grain surfaces. However, the presence of nano- and microphase gold particles embedded in the clayey masses suggests that gold does not necessarily re-precipitate directly back onto the grain surface. Kaolinite-micaceous clayey masses and Fe, Ti oxyhydroxides can act as a substrate for the adsorption of colloidal gold nanoparticles and soluble gold complexes that were subsequently reduced to nanophase colloids (Ran et al., 2002; Hong et al., 2006; Zhu et al., 2009; Shuster et al., 2017). Overgrowths of nanosized, 'a high fineness' gold in a paragenesis with clayey masses filling concavities within the studied grain surfaces could have been produced through this process.

Rare seed and layer by layer growths of exceedingly a high fineness gold noted directly on the surfaces of primary grains can represent authigenic gold precipitated from externally derived complexing aqueous solutions. Precipitation may result from changes in solution chemistry or catalysis by solids, of which free gold is among the most effective ones (McCready et al., 2003; Kalinin et al., 2009; Shuster and Southam, 2015; Kirillov et al., 2016).

In the Wądroże unit, the absence of noticeable dispersed gold in the kaolinite-hydromica weathering cover (Janczyszyn and Wyszomirski, 1986; Wierchowiec, 2010) suggests limited migration of complexing solutions and points to internally derived gold re-precipitation.

However, the occurrence of bacteriomorphic aggregates and coral-like gold that grow on the surface of the primary grain indicates that auriferous colloids took part in the deposition and redistribution of gold in artificial, technogenous sections.

The ability of sulfur-oxidizing and sulfur-reducing bacteria to transform gold complexes into nano- and microscopic-sized gold particles (Lengke and Southam, 2005, 2007; Lengke et al., 2006; Reith et al., 2007) suggests that under certain supergene conditions, bacteria contribute to the formation of authigenic gold. Based on the evidence presented by the above mentioned workers, a bacterial origin cannot be precluded for at least some of the bubbly and clustered aggregates identified within the historically mined gold deposits of Wądroże Wielkie.

In a number of early studies, the morphology of gold grains that display 'bacterioform' textures has been used as evidence for microbial gold precipitation and biomineralization in the placer environment (e.g., Bischoff et al., 1992; Reith et al., 2006, 2010; Fairbrother et al., 2012; Shuster et al., 2015, 2017). However, analogous gold morphologies were also produced abiotically (Knight, 1993; Watterson, 1994), and therefore morphology alone cannot be used as adequate evidence of bacterial involvement in the formation of authigenic gold.

The analysis of the available materials shows that the main problem in the evaluation of the extent of gold mobility in the surficial environment, as well as the extent of authigenic growth of gold within the host sediments of placer deposits lies in the determination of specific features of transitional forms of primary gold particles and is indicative of redeposited authigenic gold.

Advancing chemical weathering induces morphological and chemical changes of primary gold particles. At first, partial dissolution produces microscopic pits at the surfaces of gold particles, which leads to the development of a spongy inner texture (Mann, 1984; Wilson, 1984; Santosh and Omana, 1991; Knight et al., 1999). The intensification of dissolution processes may induce the microdivision of the primary gold grain. The resulting particles, continuously subjected to a chemical attack by supergene solutions, become smaller and smaller (until their probable complete dissolution). Shvartsev and Dutova (2001) examined gold mobility in the weathering cover by studying the ground waters of the Tsentral'NOE goldfields in Kuznetsk Alatau. They showed that most of the gold (c.a. 60–70%) is combined by a clayey regolith and the rest is concentrated in aqueous and/or colloidal solutions. The gold is transported and subsequently precipitated from these solutions, forming secondary authigenic gold under favourable geochemical conditions.

6. Conclusions

Well-preserved, nano- to microscopic gold overgrowths and aggregates of pure gold at Mikołajowice localities confirm gold mobility at micron and individual-grain scales and highlight the complex nature of the multi-stage processes of dissolution and gold re-precipitation in a temporary environment.

These supergene transformations determine the authigenic morphotypes of gold, defined in this study and the composition of grains in placer settings.

Importantly, gold nano-particle formation and aggregation, as well as the surface morphologies of the studied gold grains are the result of the current supergene dissolution, redeposition and re-precipitation in technogenous profiles occurring over historic rather than geological periods.

A mode of growth of the nanoparticles has been observed during the nano- to microtextural investigations of gold grains, from the isolated semi-spherical nanoparticles, agglomerates to irregularly shaped plates of gold.

Rare seed-like gold overgrowths, bubble-like protrusions as well as aggregates of coral- and plate-like gold morphotypes are well preserved, lacking any signs of physical damage, and they seem to be indicative of the neoformation and aggregation of authigenic gold.

In conclusion, the identification of these specific authigenic morphotypes of gold supports the assessment of the scale of supergene modification and formation of authigenic gold in the physicochemically unstable environment of technogenous deposits disturbed by repeated historical mining activities.

Acknowledgments

The part of analytical work was supported by the PGI-NRI internal grant no. 61.6101.1601.00.0. for S. Mikulski. The authors would thank the reviewers – Dr. Vladimir Naumov and an anonymous reviewer for very detailed and constructive comments, which greatly improved the final version of this manuscript.

Appendix A. Supplementary data

Supplementary data associated with this article can be found, in the online version, at https://doi.org/10.1016/j.oregeorev.2018.07.009.

References

Badura, J., Przybylski, B., 2004. Evolution of the Late Neogene and Eopleistocene fluvial system in the Foreland of Sudetes Mountains, SW Poland. Annales Societatis Geologorum Poloniae 74, 43–61.

Berezowska, B., Berezowski, Z., 1979. Detailed geological map of the Sudetes at scale 1:25 000, the Wądroże Wielkie sheet. Wydawnictwa Państwowego Instytutu Geologicznego, Warszawa.

Bischoff, G.C.O., Coenraads, R.R., Lusk, J., 1992. Microbial accumulation of gold: an example from Venezuela. Neues Jahrbuch für Geologie und Paläontologie, Abh. 185, 131–159.
Cao, J., Hu, R., Liang, Z., Peng, Z., 2009. TEM observations of geogas-carried particles from the Chankeng concealed gold deposit, Guangdong Province, South China. J. Geochem. Explor. 101, 247–253.
Cobley, C.M., Xia, Y., 2009. Gold and nano-technology. Elements 5, 309–313.
Clough, D.M., Craw, D., 1989. Authigenic gold-marcasite association: evidence for nugget growth by chemical accretion in fluvial gravels, southland, New Zealand. Economic Geol. 84, 953–958.
Craw, D., MacKenzie, D., Grieve, P., 2015. Supergene gold mobility in orogenic gold deposits, Otago Schist, New Zealand. N. Z. J. Geol. Geophys. 58 (2), 123–136.
Cwojdziński, S., Żelaźniewicz, A., 1995. The crystalline basement of the Fore-Sudetic Block. Rocznik PTG, Guide to excursions LXVI Annual Meeting of Polish Geological Society. pp 11–27 (in Polish). Wrocławska Drukarnia Naukowa, Wrocław.
Desborough, G.A., 1970. Silver depletion indicated by microanalysis of gold from placer occurrences, Western United States. Econ. Geol. 65, 304–311.
Domaszewska, T., 1964. Occurrence and exploitation of gold in Lower Silesia. Przegląd Geol. 12 (4), 180–185.
Fairbrother, L., Brugger, J., Shapter, J., Laird, J., Southam, G., Reith, F., 2012. Supergene gold transformation: biogenic secondary and nano-particulate gold from arid Australia. Chem. Geol. 320–321, 17–31.
Falconer, D.M., Craw, D., 2009. Supergene gold mobility; a textural and geochemical study from gold placers in southern New Zealand. Soc. Econ. Geol. 14, 77–93.
Friese, F.W., 1931. The transportation of gold by organic underground solutions. Econ. Geol. 26 (4), 421–431.
Freyssinet, P., Butt, C.R.M., Morris, R.C., Piantone, P., 2005. Ore-forming processes related to lateritic weathering. Econ. Geo. 681–722.
Greffié, C., Benedetti, M., Parron, C., Amouric, M., 1996. Gold and iron oxide associations under supergene conditions: an experimential approach. Geochim. et Cosmoch. Acta 60, 1531–1542.
Grocholski, A., 1986. The Proterozoic and Palaeozoic in the south-western Poland in a light of a new data. Biuletyn Instytutu Geologicznego 355, 7–29.
Grodzicki, A., 1966. Auriferous sands from Legnickie Pole – Mikołajowice. Wądroże Wielkie [Eng. Sum.]. Archiwum Mineralogiczne 26 (1/2), 473–497.
Groen, J.C., Craig, J.R., Rimstidt, J.D., 1990. Gold-rich rim formation on electrum grains in placers. Can. Mineral. 28, 207–228.
Hefton, K., 1999. Sudety Regional Study – Completion Report. National Geological Archive, PGI-NRI, Warszawa, Poland exploration program, Homestake.
Hong, H., Tie, L., 2005. Characteristics of the minerals associated with gold in the Shewushan supergene gold deposit, China. Clays Clay Miner. 53, 162–170.
Hong, H., Tie, L., Bian, Q., Zhou, Y., 2006. Interface characteristics between colloidal gold and kaolinite surface by XPS. J. Wuhan Univ. Technol., Mater. Sci. Ed. 21 (3), 90–93.
Hough, R.M., Butt, A.R.M., Reddy, S.M., Verrall, M., 2007. Gold nuggets: supergene or hypogene. Aust. J. Earth Sci. 54, 959–964.
Hough, R.M., Noble, R.R.F., Hitchen, G.J., Hart, R., Reddy, S.M., Saunders, M., Clode, P., Vaughan, D., Lowe, J., Gray, D.J., Anand, R.R., Butt, C.R.M., Verrall, M., 2008. Naturally occurring gold nanoparticles and nanoplates. Geology 36, 571–574.
Hough, R.M., Noble, R.R.P., 2010. Colloidal gold nanoparticles in ore systems. Geochim. Cosmochim. Acta 74, A420.
Hough, R.M., Reich, M., Noble, R.R.P., 2011. Noble metal nanoparticles in ore systems. Ore Geol. Rev. 42, 55–61.
Janczyszyn, J., Wyszomirski, P., 1986. Gold in kaolin from Wądroże Wielkie (Lower Silesia, Poland). In: Tenth Conference on clay mineralogy and petrology, 261-266, Ostrava.
Kalinin, Yu.A., Kovalev, K.R., Naumov, E.A., Kirillov, M.V., 2009. Gold in the weathering crust at the 'Suzdal' deposit (Kazakhstan). Russ. Geol. Geophys. 50, 174–187.
Kanasiewicz, J., 1982. A method of quantitative interpretation of schlichs alluvial anomalies on the example of gold (in Polish with English summary). Przegląd Geologiczny 30 (8), 404–406.
Kerr, G., Craw, D., 2017. Mineralogy and geochemistry of biologically-mediated gold mobilization and redeposition in a semiarid climate, southern New Zealand. Minerals 7 (147), 1–18.
Kim, H., Kim, Y.H., Joo, J.B., Ko, J.W., Yi, J.H., 2009. Preparation of coral-like porous gold for metal ion detection. Microporous Mesoporous Mater. 122, 283–287.
Kirillov, M.V., Bortnikova, S.B., Gaskova, O.L., 2016. Authigenic gold formation in the cyanidation tailings of gold–arsenopyrite–quartz ore of Komsomolsk deposit (Kuznetski Alatau, Russia). Environ. Earth Sci. 75 (1050), 1–11.
Knight, J., 1993. Preliminary evidence for the involvement of budding bacteria in the origin of Alaskan placer gold. Geology 21, 279–280.
Knight, J., Morison, S., Mortensen, J., 1999. The relationship between placer gold particle shape, rimming, and distance of fluvial transport as exemplified by gold from the Klondike District, Yukon Territory. Canada. Econ. Geol. 94, 635–648.
Koneev, R.I., 2006. Nanomineralogy of gold epithermal deposits in the Chatcal-Kurama region (Uzbekistan). St. Petersburg. DELTA 2006, 218.
Lengke, M.F., Fleet, M.E., Southam, G., 2006. Morphology of gold nanoparticles synthesized by filamentous cyanobacteria from gold(I)-thiosulfate and gold(III)-chloride complexes. Langmuir 22, 2780–2787.
Lengke, M.F., Southam, G., 2005. The effect of thiosulfate-oxidizing bacteria on the stability of the gold-thiosulfate complex. Geochim. et Cosmochim. Acta 69, 3759–3772.
Lengke, M.F., Southam, G., 2006. Bioaccumulation of gold by sulfate-reducing bacteria cultured in the presence of gold(I)-thiosulfate complex. Geochim. et Cosmochim. Acta 70, 3646–3661.
Lengke, M.F., Southam, G., 2007. The deposition of elemental gold from gold(I)-thiosulfate complexes mediated by sulfate-reducing bacterial conditions. Econ. Geol. 102 (1), 109–126.
Mann, A.W., 1984. Mobility of gold and silver in lateritic weathering profiles: Some observations from Western Australia. Econ. Geol. 79, 35–49.
McClenaghan, M.B., 2014. Overview of indicator mineral recovery methods for sediments and bedrock. Application of indicator mineral methods to mineral exploration. In: McClenaghan, M.B., Plouffe, A., D. Layton-Matthews (Eds.), Geological Survey of Canada. Open File, pp. 1–8.
McCready, A.J., Parnell, J., Castro, L., 2003. Crystalline placer gold from the Rio Neuquén, Argentina: implications for the gold budget in placer gold formation. Econ. Geol. 98, 623–633.
Migon, P., 1997. Crystalline rock inselbergs in southwestern Poland. Origin and palaeoenvironmental significance. Acta Universitatis Wratislaviensis, Studia Geograficzne 1872 (66), 1–102.
Mikulski, S.Z., Wierchowiec, J., 2013. Placer scheelite and gold from alluvial sediments as indicators of the primary mineralization – examples from the Sudetes and Fore-Sudetic Block (Lower Silesia region, SW Poland). Geol. Quarterly 57, 503–514.
Naumova, O.B., Naumov, V.A., Osovetsky, B.M., Lunev, B.S., Kovin, O.N., 2013. Nanoforms of secondary gold in the tailings wastes: placers of is River, Russia. Middle East J. Sci. Res. 18 (3), 316–320.
Oliveira, S.M., Larizzatti, J.H., 2006. Some observations on gold in the weathering profile at Garimpo Porquinho, an artisanal mine in the Tapajós region, Brazilian Amazon. Geologia USP Série Cientifica 5 (2), 1–11.
Osovetsky, B.M., 2016. Aggregation of nanogold particles in the environment. Nat. Resour. Res. 25 (2), 241–253.
Osovetsky, B.M., 2012. Nanosculpture of gold surface. Perm: Perm State University Press. (in Russian). p. 232.
Osovetsky, B.M., 2013. Natural nanogold. Perm: Perm State University Press. (in Russian). p. 176.
Palenik, C.S., Utsunomiya, S., Reich, M., Kesler, S.E., Wang, L.M., Ewing, R.C., 2004. 'Invisible' gold revealed: Direct imaging of gold nanoparticles in a Carlin-type deposit. Am. Mineral. 89, 1359–1366.
Quiring, H., 1913. Über das Goldvorkommen bei Goldberg in Schlesien und seine bergmännische Gewinnung im 13 und 14 Jahrhundert. Schlesische Gesellschaft für Vaterländische Cultur 91, 56–89.
Ran, Y., Fu, J., Rate, A.W., Gilkes, R.J., 2002. Adsorption of Au (I, III) complexes on Fe, Mn oxides and humic acid. Chem. Geol. 185, 33–49.
Reith, F., Rogers, S.L., McPhail, D.C., Webb, D., 2006. Biomineralization of gold: biofilms on bacterioform gold. Science 313 (5784), 233–236.
Reith, F., Lengke, M.F., Falconer, D., Craw, D., Southam, G., 2007. The geomicrobiology of gold. ISME J. 1 (7), 567–584.
Reith, F., Fairbrother, L., Nolze, G., Wilhelmi, O., Clode, P.L., Gregg, A., Parsons, J.E., Wakelin, S.A., Pring, A., Hough, R., Southam, G., Brugger, J., 2010. Nanoparticle factories: Biofilms hold the key to Au dispersion and nugget formation. Geology 38, 843–846.
Reith, F., Stewart, L., Wakelin, S.A., 2012. Supergene gold transformation: secondary and nanoparticulate gold from southern New Zealand. Chem. Geol. 320, 32–45.
Santosh, M., Omana, P.K., 1991. Very high purity gold from lateritic weathering profiles of Nilambur, southern India. Geology 19 (7), 746–749.
Sawicki, L., Teisseyre, H., 1978. Geological Map of the Lower Silesia (Without Quaternary Sediments) at Scale 1:500 000. Zakład Narodowy im, Ossolińskich, Wrocław.
Shuster, J., Southam, G., 2015. The in-vitro 'growth' of gold grains. Geology 43 (1), 79–82.
Shuster, J., Johnston, C.W., Magarvey, N.A., Gordon, R.A., Barron, K., Banerjee, N.R., Southam, G., 2015. Structural and chemical characterization of placer gold grains: implications for bacterial contributions to grain formation. Geomicrobiological J. 32 (2), 158–169.
Shuster, J., Reith, F., Cornelis, G., Parsons, J.E., Parson, J.M., Southam, G., 2017. Secondary gold structures: relics of past biogeochemical transformations and implications for colloidal gold dispersion in subtropical environments. Chem. Geol. 450, 154–164.
Shvartsev, S.L., Dutova, E.M., 2001. Hydrochemistry and mobilization of gold in the hypergenesis zone (Kuznetsk Alatau, Russia). Geol. Ore Deposits 43 (3), 224–233.
Watterson, J.R., 1994. Artifacts resembling budding bacteria produced in placer gold amalgams by nitric acid leaching. Geology 22 (12), 1131–1134.
Webster, J.G., 1986. The solubility of Au and Ag in the system Au-Ag-S-O_2-H_2O at 25 °C and 1 atm. Geochim Cosmochimica Acta 1986 (50), 245–255.
Webster, J.G., Mann, A.W., 1984. The influence of climate, geomorphology and primary geology on the supergene migration of gold and silver: Jour. Geochem. Explor. 22, 21–42.
Wierchowiec, J., 2010. Gold in technogenous placers of Lower Silesia, Poland. Warsaw University Press, pp. 1–206.
Wierchowiec, J., 2011. Placer gold of East Sudetes and its foreland, Poland. In: Kozlowski, A., Mikulski, S.Z. (Eds.), Gold in Poland. Archivum Mineralogiae Monograph, pp. 209–242.
Wilson, A.F., 1984. Origin of quartz-free gold nuggets and supergene gold found in laterites and soils. A review and some new observations. Aust. J. Earth Sci. 31, 303–316.
Zhu, L., Letaief, S., Liu, Y., Gervais, F., Detellier, C., 2009. Clay mineral-supported gold nanoparticles. Appl. Clay Sci. 43 (3–4), 439–446.
Zhmodik, S.M., Kalinin, Y.A., Roslyakov, N.A., Mironov, A.G., Mikhlin, Y., Belyanin, D.K., et al., 2012. Nanoparticles of noble metals in the supergene zone. Geol. Ore Deposits 54 (2), 141–154.
Zöller, A., Heuseler, E., 1926. Die Goldquarzgänge und Goldseifen zwischen Grosswandriss und Wahlstatt in Niederschlesien. Glückauf 48, 1585–1588.